# A 1D coordination polymer built on asymmetric $\mu$1,1,3-azide bridge: from unusual topology to magnetic properties and Cu(II)/Cu(I) redox reversibility

Jean-Bernard Tommasino, Guillaume Chastanet, Boris Le Guennic, Vincent Robert, Guillaume Pilet

NJC

Cite this: *New J. Chem.*, 2012, **36**, 2228–2235

www.rsc.org/njc

**PAPER**



# A 1D coordination polymer built on asymmetric $\mu_{1,1,3}$-azide bridge: from unusual topology to magnetic properties and Cu(II)/Cu(I) redox reversibility†

**Jean-Bernard Tommasino,*[a] Guillaume Chastanet,[b] Boris Le Guennic,*[cd] Vincent Robert[ce] and Guillaume Pilet[a]**

***Received (in Montpellier, France) 26th January 2012, Accepted 3rd August 2012***
**DOI: 10.1039/c2nj40302a**

An azide-bridged Cu(II) one dimensional polymer was synthesized in a one pot reaction in the presence of ammonia. The refined crystal structure evidenced the unusual asymmetric $\mu_{1,1,3}$ coordination mode of the azide ion leading to a $\{Cu(\mu_{1,1,3}\text{-}N_3)(\mu_1\text{-}N_3)(NH_3)_{0.8}(H_2O)_{1.2}\}_n$ chain. The redox process of this complex was studied by cyclic voltammetry evidencing the Cu(II)/Cu(I) reversibility. Magnetic measurements were interpreted as a uniform antiferromagnetic chain ($J = -15.2$ cm$^{-1}$) holding rather strong inter-chain exchange ($zJ' = -2.8$ cm$^{-1}$). Multireference difference dedicated configuration interaction (DDCI) calculations confirmed the non-negligible intensity of inter-chain interactions and evidenced a strong influence of the type of coordinated solvent, $NH_3$ or $H_2O$, on the nature and magnitude of the magnetic exchange.

## Introduction

The azide bridge has been known for a long time for its ability to generate molecular architectures of high nuclearity. In particular, its versatility as a magnetic coupler was deeply investigated. For instance, many studies deal with the relation between the molecular structure and the magnetic behaviour,[1–5] as well as the possible occurrence of Single Molecule Magnet (SMM) and Single Chain Magnet (SCM) behaviours.[6,7] Therefore, many structures have already been described in the literature with the azide ligand used as a molecular bridge and a magnetic relay. Indeed, the $N_3^-$ ligand presents several common coordination modes. Besides the most frequently encountered *end-to-end* ($\mu_{1,3}$-$N_3$, **EE**) and *end-on* ($\mu_{1,1}$-$N_3$, **EO**) double coordination modes (Scheme 1),[1–4] single $\mu_{1,1}$ and $\mu_{1,3}$,[8] triple $\mu_{1,1,1}$[9] and $\mu_{1,1,3}$,[10] or quadruple $\mu_{1,1,1,1}$[11] and $\mu_{1,1,3,3}$[12] connection forms were encountered. This ability to coordinate up to six metal ions leads to structural varieties of azide-complexes that range from molecular clusters[6] to multidimensional materials (1D, 2D and 3D).[1–5,7–12] Moreover, different bridging modes of the azide ion may simultaneously exist in the same species, leading to original alternating topologies and magnetic behaviours exemplified by the widespread $\{$**EO–EE**$\}_n$ sequence[1–4] and the less common, $\{$**EO–EE–EE**$\}_n$, $\{$**EO–EO–EO–EE**$\}_n$, $\{$**EO–EO–EO–EO–EE**$\}_n$ chain assemblies.[3,4,13] Even more exotic sequences were reported when single, double and triple bridges are present simultaneously. Finally, the coordination pattern could be either symmetric, with all equivalent metal–azide bond lengths, or may deviate from such a perfect picture (Scheme 1).

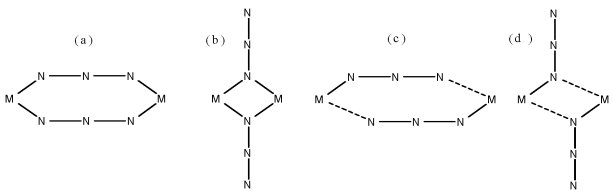


**Scheme 1** Symmetric **EE** (a) and **EO** (b) and asymmetric **EE** (c) and **EO** (d) double coordination modes usually encountered for the azide ligand.

It is known that magnetic properties are influenced by the complex topology. From magneto-structural correlations, based on both experimental[14] and theoretical[15] studies, some general trends were evidenced for double-bridged species: the **EE** mode favours antiferromagnetic interactions whereas the **EO** one generally leads to ferromagnetic exchange. These studies also highlight the great sensitivity of the magnetic exchange coupling to specific structural parameters such as the metal–azide–metal angles or the asymmetry in the coordination mode of the azide bridges.[16]

[a] *Laboratoire des Multimatériaux et Interfaces (LMI), UMR 5615, CNRS-Université Claude Bernard Lyon 1, bâtiment Berthollet, Avenue du 11 novembre 1918, 69622 Villeurbanne cedex, France. E-mail: jbtomasi@univ-lyon1.fr*
[b] *CNRS, Université de Bordeaux, ICMCB, 87 avenue du Dr. A. Schweitzer, Pessac, F-33608, France*
[c] *Laboratoire de Chimie, UMR CNRS 5182, Ecole Normale Supérieure de Lyon, 46 allée d'Italie, 69364 Lyon cedex 07, France*
[d] *Sciences Chimiques de Rennes, UMR 6226, CNRS - Université de Rennes 1, 35042 Rennes Cedex, France*
[e] *Laboratoire de Chimie Quantique, UMR 7177, Université de Strasbourg, 4 rue Blaise Pascal, 67000 Strasbourg, France*

† Electronic supplementary information (ESI) available: CCDC 862144. For ESI and crystallographic data in CIF or other electronic format see DOI: 10.1039/c2nj40302a

 

As part of our work on the design of molecular magnetic architectures, various mono-dimensional coordination polymers based on azide ligands were obtained such as original topologies with Cu(II) ions linked by single azide bridge.[5,8c,17] Along this work, the use of the azide ion in conjunction with a Cu(II) salt and ammonia led to a chain characterized by X-ray diffraction. The general formula $\{Cu(\mu_{1,1,3}\text{-}N_3)(\mu_1\text{-}N_3)(NH_3)_{0.8}(H_2O)_{1.2}\}_n$ reveals an unusual topology and statistical distribution of water and ammonia along the chain. Electrochemical investigations demonstrate the reversibility of the Cu(II)/Cu(I) redox process and the stability of the Cu(I) phase. The magnetic properties are investigated through solid state characterization and *ab initio* configuration interaction (CI) calculations. A net antiferromagnetic behaviour is experimentally observed and the impact of the coordinated solvent molecules on the exchange coupling constants is theoretically analyzed.

## Results and discussion

### Synthesis

The formation of the complexes is based on the complexation of equilibra with ammonia in aqueous solution as illustrated in a previous article (Scheme 2).[18] The ammonia added in large excess favours first the formation of the soluble ammonia–Cu(II) complex, even in the presence of $N_3^-$. Indeed, the UV visible of the solution mixture after one hour shows a band at 640 nm characteristic of the Cu(II)–ammonia complex (see Fig. S1, ESI†). Later, due to the evaporation of the ammonia and methanol solvent, and among the possible reactions, an equilibrium competition takes place between the formation of the ammonia–Cu(II) and the azide–Cu(II) complexes in favour of the second one. At this stage, the band at 640 nm decreases. After five days, the visible signal becomes characteristic of the azide–Cu(II) complex. So, the slow formation of the azide–Cu(II) complex allows then the obtention of green single-crystals suitable for X-ray diffraction characterizations. From these results, we can propose the following general mechanism:

$$Cu^{2+} + 4\,NH_3 \underset{(1)}{\overset{CH_3OH/H_2O}{\rightleftharpoons}} [Cu(NH_3)_4(H_2O)_2]^{2+}$$

$$n\,[Cu(NH_3)_4(H_2O)_2]^{2+} + 2n\,N_3^- \underset{(2)}{\overset{H_2O}{\rightleftharpoons}} \{Cu(N_3)_2(NH_3)_{2-x}(H_2O)_x\}_n + (2+x)n\,NH_3$$

**Scheme 2** Proposed synthetic mechanism for the polymer formation.

### Crystal structure description

The asymmetric unit can be described as a Cu(II) ion coordinated by two azide ligands, one acting as a bridge between the metal centres, the other one being in a $\mu_1$ coordination mode. The bridging $N_3^-$ ion exhibits a $\mu_{1,1,3}$ coordination mode linking three Cu(II) ions to grow a 1D polymer running along the *a*-axis of the unit-cell (Fig. 1). The coordination polyhedron of the metal centre is completed perpendicularly to the chain by two solvent molecules that can be either ammonia or water. Indeed, the determination of the solvent nature by X-ray diffraction appears to be hazardous since (i) the electron number difference between oxygen and nitrogen atoms is too small, and (ii) refinements with only $H_2O$ or only $NH_3$ as coordinated solvent are both very satisfactory, resulting in two

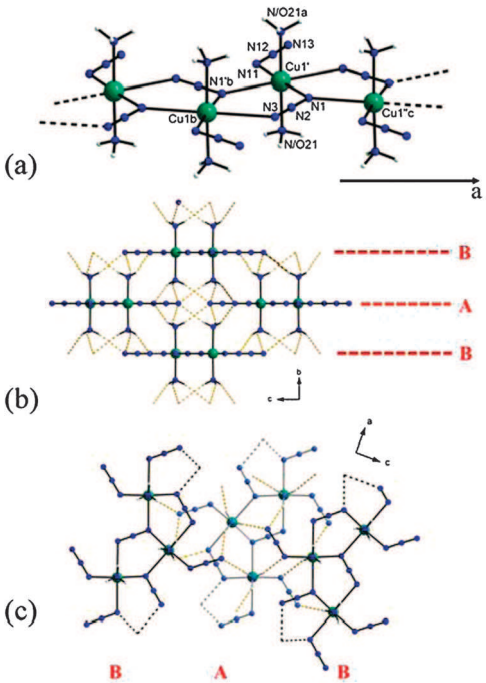


**Fig. 1** (a) $\{Cu(\mu_{1,1,3}\text{-}N_3)(\mu_1\text{-}N_3)(solvent)_2\}_n$ 1D polymer running along the *a*-axis of the unit-cell with important labels. Atoms with *a*, *b* or *c* labels are generated with the following transformations respectively: *a* (*x*,1.5 − *y*,*z*), *b* (−0.5 + *x*,1.5 − *y*,1.5 − *z*) and *c* (0.5 + *x*,1.5 − *y*,1.5 − *z*); (b) representation of the packing cohesion in the (*b*,*c*)-plane of the unit-cell. The hydrogen bonds are represented by dashed brown lines; (c) a second representation of the packing cohesion with B and shifted A planes.

acceptable solutions $\{Cu(\mu_{1,1,3}\text{-}N_3)(\mu_1\text{-}N_3)(NH_3)_2\}_n$ and $\{Cu(\mu_{1,1,3}\text{-}N_3)(\mu_1\text{-}N_3)(H_2O)_2\}_n$. A powerful technique to evaluate the chemical composition of a compound is the CHN elemental analysis that determines the weight contribution of carbon, hydrogen and nitrogen atoms. Regarding the two possible solutions, a huge difference is expected in the hydrogen and nitrogen elemental weight contribution. Indeed, with ammonia, the $CuH_6N_8$ formula leads to percentages of H = 3.34% and N = 61.89% whereas with water, $CuH_4N_6O_2$, H = 2.20% and N = 45.92%. Elemental analysis was thus performed on a polycrystalline sample to discriminate between these two solutions, taking care of the explosive nature of azide. The experimental values of 52.39% of nitrogen and 2.94% of hydrogen indicate that the synthesized compound presents a mixture of solvent molecules close to a 1/3 $NH_3$ : 2/3 $H_2O$ ratio. The refined formula extracted from the elemental analysis is then $\{Cu(\mu_{1,1,3}\text{-}N_3)(\mu_1\text{-}N_3)(NH_3)_{0.8}(H_2O)_{1.2}\}_n$. Based on these results, a new refinement of the crystal structure was undertaken using a statistical distribution of ammonia and water with good agreement factors (see Experimental section) and for simplicity, the crystal structure description will be conducted using the following denomination: $\{Cu(\mu_{1,1,3}\text{-}N_3)(\mu_1\text{-}N_3)(solvent)_2\}_n$.

In the crystal view of the chain, the Cu(II) ion is located in a distorted octahedral environment composed of four azide ligands in the square base plane and two coordinated solvent molecules ($NH_3$ or $H_2O$) located at the apical positions (Fig. 1). The first azide moiety is mono-coordinated (N11, N12 and N13)

while the second one (N1, N2 and N3) links one copper cation to two other ones through a $\mu_{1,1,3}$ coordination mode (Fig. 1). Two adjacent Cu ions in the chain are linked through a rather uncommon double azide-bridge: one **EO** and one **EE** (Scheme 3). This dimeric unit is characterized by two short Cu1–N1′ and Cu1′–N1 (2.062(2) Å) and two long Cu1–N3 and Cu1′–N1′ (2.644(2) Å and 2.533(2) Å) bond lengths. The Cu1–N1′–Cu1′ angle $\theta$ of 134.06° induces a separation of 4.24 Å between the Cu(II) centres. Cu1 is also connected to a second Cu(II) neighbour Cu1′′ through a single *end-to-end* bridging mode characterized by the two long Cu1–N3 and Cu1′′–N1 bond lengths (2.644(2) Å and 2.533(2) Å, respectively). This induces a distance of 6.38 Å between the metal centres.

Only a few examples of such a type of topology with only azide linkers are reported in the literature. Indeed, most of the architectures based on $\mu_{1,1,3}$ coordination mode are constructed on alternating **EE–EO** chains.[10b,d–h] Moreover, only a couple of $\{Cu(\mu_{1,1}\text{-}N_3)(\mu_{1,3}\text{-}N_3)Cu\}$ dimeric units which exhibit simultaneously **EE** and **EO** coordination modes (Scheme 3) are known.[10c,19] In that sense, this makes the title compound an original member of the wide family of azide-based polymers.

The structural cohesion is guaranteed by hydrogen bonds built from hydrogen atoms of coordinated solvent molecules ($NH_3$ or $H_2O$) and nitrogen atoms of $N_3$ bridges between different chains from two different planes (Fig. 1b). The whole structure can then be viewed as layers (planes A and B), in the (*a*,*c*)-plane of the unit-cell, of $\{Cu(N_3)_2(solvent)_2\}_n$ polymers. In order to avoid steric hindrance, the chains in plane A are shifted along the *a*-axis of the unit-cell compared to those in plane B. The shortest inter-chain distances in the directions [011] (between chains in plans A and B), [010] (between chains in plans A and A′, or B and B′) and [001] (chains in the same plan) are equal to 5.90 Å, 7.44 Å and 10.42 Å, respectively. Let us note that a correct description of the hydrogen-bonding network should account for 60% of water molecules and 40% of ammonia as solvent. Nevertheless, whatever the solvent, at least one inter-chain Cu–Cu distance (5.90 Å) is comparable to the intra-chain ones (4.24 Å and 6.38 Å).

## Electrochemical studies

Despite the huge interest on Cu(II)/Cu(I) electron transfer processes in biological systems,[20] only a few studies were carried out on Cu(II) complexes based on azide linkers.[17,21] It probably mainly follows on from the interest in its magnetic coupler ability.

In order to check the occurrence of redox processes, the stability of the intermediate species and the reversibility of the global electrochemical behaviour, the title compound was carefully studied (see Experimental section). First, the electrochemical behaviours of the azide ligand and the Cu(II) salt were controlled separately in DMF. The electrochemical behaviour[20] of the $N_3^-$ ligand corresponds to an irreversible oxidation wave located at 1.40 V/SCE (Saturated Calomel Electrode). The Cu(II) salt exhibits a quasi-reversible reduction peak at −0.18 V/SCE followed by a second reduction step at −0.55 V/SCE. The latter is associated with an anodic re-dissolution peak at +0.20 V/SCE.

The voltammogram of the $\{Cu(N_3)_2S_2\}_n$ chain (S stands for the solvent molecules) is characterized by a reversible behaviour at $E_{1/2}$ = 0.04 V/SCE (Fig. 2) and the exhaustive electrolysis performed at −0.50 V/SCE exhibits a mono-electronic reduction accompanying a change in the solution colour from dark orange to light yellow. A second reduction step at −1.05 V/SCE can be observed and is associated with a typical anodic re-dissolution peak of Cu(0) at −0.30 V/SCE. From these observations, the electrochemical mechanism can be summarized as follows (Scheme 4):

The potentials observed for the polymer slightly differ from those of the single Cu(II) and $N_3^-$ species, demonstrating the stability of the azide–Cu(II) complex in DMF solution (no decomposition observed).

At this stage as well as for many complexes in solution, our electrochemistry studies cannot demonstrate that the polymer chain which was determined by X-ray diffraction in the solid state remains identical in DMF solution. Several processes can be anticipated in solution, as for example salvation, ligand/solvent exchanges. However, our electrochemical results show that a single Cu(II) azido complex, different from free Cu(II) ions is present in DMF solution. Moreover, the azide Cu(II)/Cu(I) complexes seem stable in organic solvent under an inert atmosphere, its $Cu^{II}/Cu^{I}$ reversibility becomes interesting for redox catalysis applications. In that context, we attempted to study its behaviour in the absence and in the presence of dioxygen by electrochemical-UV-Visible measurements. The UV-Visible spectrum (Fig. 3) recorded before electrolysis shows a $\lambda_{max}$ equal to 419 nm with a molar extinction coefficient $\varepsilon$ equal to 3410 L mol$^{-1}$ cm$^{-1}$. A weaker band can be also observed at $\lambda_{max}$ equal to 620 nm. Afterward, we shall focus our electrochemical-UV visible study at 420 nm (Fig. 3).

A decrease in the absorbance is observed with increasing charge quantities recorded. As the difference absorbance $A_0 - A$ ($A_0$: initial absorbance; $A$: absorbance during the electrolysis) is

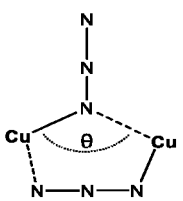


**Scheme 3** Asymmetric **EE**/**EO** coordination modes encountered in the title compound.

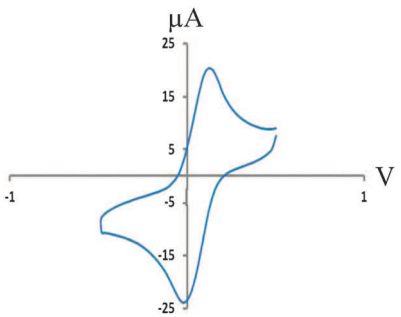


**Fig. 2** Cyclic voltammogram of the title compounds in DMF at 0.1 V s$^{-1}$ at a glassy carbon electrode restricted to the reversible system.

 

$$\{Cu^{II}\text{-}(N_3)_2\} \overset{e^-}{\rightleftharpoons} \{Cu^{I}\text{-}(N_3)_2\} \xrightarrow{e^-} Cu^0 + 2N_3^-$$

**Scheme 4** Principle of the redox processes at the glassy carbon electrode in DMF solvent.

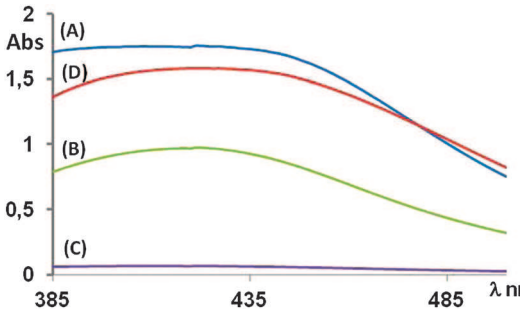


**Fig. 3** UV-Visible spectra of $\{Cu(N_3)_2S_2\}_n$; 0.5 mM at different electrolysis steps; (A) $Q = 0$ F mole$^{-1}$; (B) $Q = 0.4$ F mole$^{-1}$; (C): $Q = 0.9$ F mole$^{-1}$; (D): after 15 min under an air atmosphere.

proportional to the concentration ratio $Q/Q_0$ ($Q_0$: electricity quantities for one electron transfer by mole; $Q$: electricity quantities recorded during the coulometry) during the electrolysis, it demonstrates the absence of a complicated mechanism. After electrolysis, the solution containing the Cu(I) polymer is stirred under an air atmosphere for 15 minutes and its colour (light yellow) returns to the initial one (dark orange). The UV-Visible spectrum is then characteristic of the initial $\{Cu^{II}(N_3)_2(solvent)_2\}_n$ polymer. This phenomenon can be interpreted as a reaction of the $\{Cu^{I}(N_3)_2(solvent)_2\}_n$ polymer with dioxygen to generate, by electron transfer (Scheme 5), the anionic radical $O_2^{\bullet -}$ and the corresponding $\{Cu^{II}(N_3)_2(solvent)_2\}_n$ polymer. The elucidation of the kinetics parameters of this reaction is still in progress.

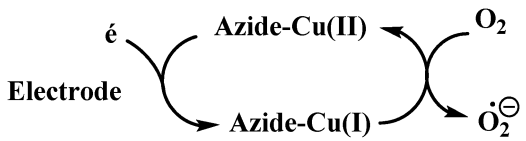


**Scheme 5** Activation mechanism of the dioxygen reduction by the $\{Cu^{II}(N_3)_2(NH_3)_2\}_n$ polymer.

## Magnetic studies

Since azide ligand exhibits an unusual topology in the title compound, the magnetic properties were measured on a polycrystalline sample and are shown in Fig. 4 as the thermal dependence of the molar magnetic susceptibility times the temperature ($\chi T$). At room temperature, the $\chi_M T$ value of 0.318 cm$^3$ K mol$^{-1}$ is slightly lower than the expected value for one Cu(II) ion (0.375 cm$^3$ K mol$^{-1}$). Upon cooling, $\chi_M T$ smoothly decreases down to 100 K and then drops down to almost zero at lower temperatures. This behaviour indicates the presence of dominant antiferromagnetic exchange interactions between the Cu(II) ions. Regarding the crystal structure, the main magnetic contribution should result from the Cu1···Cu1′ exchange interaction since it is characterized by a relatively short Cu···Cu distance (4.24 Å) and two short Cu–N bond lengths. The second neighbour magnetic exchange

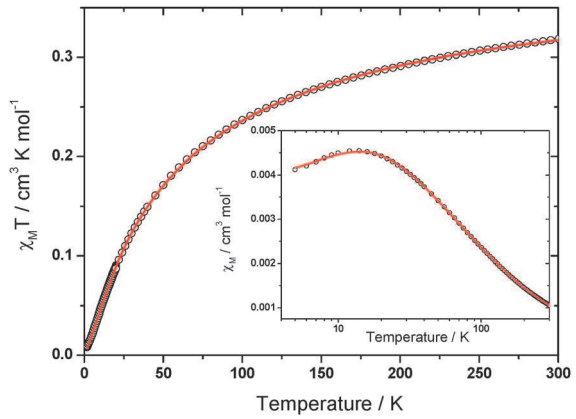


**Fig. 4** Thermal dependence of the molar magnetic susceptibility times the temperature. The straight lines stand for the fit discussed in the text.

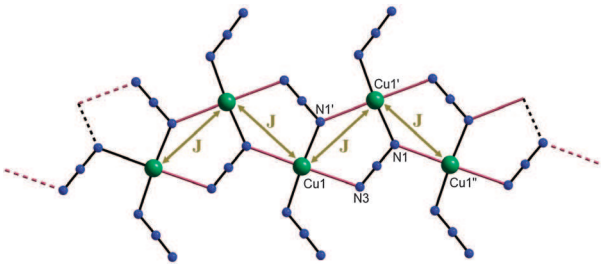


**Fig. 5** Representation of the main exchange pathway along the chain. In violet and black are represented the long and short Cu–N bonds, respectively. For clarity, coordinated solvent molecules were omitted.

between Cu1 and Cu1′′ is neglected in first approximation regarding the long Cu···Cu distance of 6.38 Å and the presence of two long Cu–N bond lengths. Therefore, the magnetic properties of the complex were first described as a uniform magnetic chain (Fig. 5). Since the global interaction appears to be antiferromagnetic, a Bonner–Fisher model[22] based on the $\hat{H} = -J\hat{S}_1 \cdot \hat{S}_2$ spin Hamiltonian is applied. The use of eqn (1) (with $X = |J|/k_BT$) fails to correctly describe the experimental curve. We therefore took into account inter-chain coupling, $J'$, which was introduced through molecular field approximation. Fig. 4 presents the best fit obtained with $J = -15.2$ cm$^{-1}$, $g = 2.01$, and $zJ' = -2.8$ cm$^{-1}$.

$$\chi_M = \frac{N_A\beta^2 g^2}{k_B T} \cdot \frac{0.25 + 0.074975X + 0.075235X^2}{1.0 + 0.9931X + 0.172135X^2 + 0.757825X^3} \quad (1)$$

The rather strong value of $zJ'$ could hinge on two different sources. The first one is clearly based on the strong hydrogen-bonding network involved in the crystal packing (Fig. 1b) with the shortest Cu···Cu distances of 5.90 Å. One chain is then connected to four (direct hydrogen bonds) or six (direct and non-direct hydrogen bonds) neighbour chains. The second one could follow from the fact that our approximation of only one exchange pathway within the chain may be too restrictive. Both solutions will be discussed thoroughly on the basis of theoretical calculations (see below).

However, let us concentrate first on the main magnetic channels. As already mentioned, the uniform antiferromagnetic chain description strongly differs from the previously reported chains exhibiting $\mu_{1,1,3}$ coordination modes of the azide-linker which were described as alternating chains of double **EE** and **EO** exchange interactions.[10] Moreover, only few {Cu($\mu_{1,1}$-$N_3$)-($\mu_{1,3}$-$N_3$)Cu} dimeric units are reported exhibiting at the same time **EE** and **EO** coordination modes (Scheme 3).[10c,19] Comparison will then be difficult to perform. However, the global antiferromagnetic exchange behaviour of the chain should result from the competition between two exchange pathways, *i.e.* along the **EO** and **EE** azide coordination modes. Nevertheless, double **EO** bridges are known to transmit ferromagnetic exchange but increasing the Cu–N–Cu angle value ($\theta$, Scheme 3) above 104° induces a change toward small antiferromagnetic values.[1–4,15] In addition, the asymmetry of the coordination mode (difference between long and short Cu–N bond lengths, Scheme 1) also contributes to favour antiferromagnetism.[10b,14f,16c,23] Finally, it has been shown that an **EO** mode associated with a mono-atomic (like hydroxo),[24] di-atomic (pyrazine)[25] and tri-atomic (azide)[19] linker contributes to increase the $\theta$ value. Since the **EO** is highly asymmetric and $\theta$ = 134°, an antiferromagnetic behaviour is expected. Conversely, double **EE** modes are known to mediate antiferromagnetic interactions which can be switched to ferromagnetic as the asymmetry of the coordination increases.[1–4,15,16] This asymmetry is rather large, favouring ferromagnetic exchange along this pathway. Therefore, one may conclude that the $J$ value of $-15.2$ cm$^{-1}$ results from this competition between the two pathways and is comparable with the $-19.6$ cm$^{-1}$ previously obtained for a similar coordination mode.[19a]

### Computational studies

The magnetic properties were further investigated by quantum chemical calculations, using wavefunction-based *ab initio* methodologies (see Computational details section). Calculations were performed on seven distinct dinuclear model complexes (Fig. 6), ensuing from the crystallographic data, without any geometry optimization. With both $NH_3$ and $H_2O$ as solvent S, two intra-chain dinuclear models are constructed, namely $\mathbf{EE/EO_S}$ and $\mathbf{EE_S}$ that correspond to Cu1···Cu1′ and Cu1···Cu1″, respectively. The modification of the solvent molecules does not affect the geometry of the core of the EE/EO units. Only the position of the solvent molecules is slightly modified through the refinement of the structures. Moreover, dinuclear models resulting from the inter-chain network are also generated in order to rationalize the high value of $zJ'$ experimentally obtained. With $NH_3$ as solvent, two dinuclear molecules are considered, corresponding to both short ($\mathbf{IS_{NH_3}}$) and long ($\mathbf{IL_{NH_3}}$) inter-chain contacts. In the case of solvent = $H_2O$, only one model is necessary ($\mathbf{IS_{H_2O}}$) due to the orientation of the hydrogen contacts in the resolved structure.

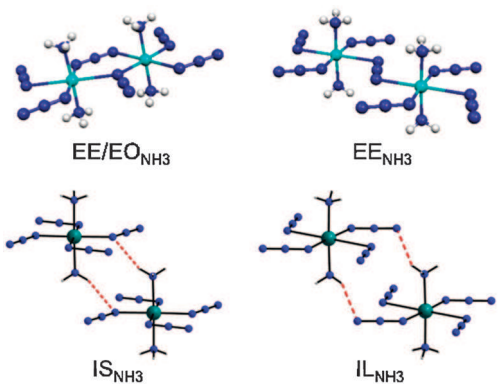


**Fig. 6** Dinuclear model complexes used in the CI calculations. The solvent is $NH_3$. Calculations with $H_2O$ as solvent were also performed.

The calculated values are compiled in Table 1. Even if such calculations do not take into account the statistical distribution of water and ammonia in the structure, they offer a pertinent view of extreme magnetic behaviours with respect to the nature of the solvent coordinated to the copper atoms. Indeed, at the best level of calculation, *i.e.* CAS(2,2) + DDCI3, it appears that changing the solvent drastically modifies the interpretation of the magnetic properties. The strongest evolution concerns the **EE**/**EO** unit that is expected to bear the main magnetic channel. Whereas the calculated $J$ value is noticeably ferromagnetic in the presence of ammonia, the situation is reversed with coordinated water molecules.

As shown in Table 1, this significantly different behaviour between the ammonia and water series already appears at the DDCI1 and CASSCF level of calculations. Nevertheless, some important modifications have been recently reported in the literature, including changes in the nature of the interaction as the level of calculations increases.[37] DDCI1 includes specific phenomena (stabilization of the ionic forms, spin polarization) which are absent at the CAS-CI level. Besides, the use of a unique set of MOs in the DDCI philosophy to investigate the singlet–triplet energy difference makes the CAS-CI or the state specific CASSCF level inappropriate. First, we anticipate the spin polarization contributions, the sign of which is difficult to anticipate, to be very similar in the two series. Indeed, these mechanisms mostly arise from the bridging part between the spin holders which is similar in both the $NH_3$ and $H_2O$ series. Secondly, the ionic forms (*i.e.*, two electrons on the same Cu centre, as opposed to neutral forms which correspond to the single occupancy of both magnetic orbitals) which are present in the singlet state, absent in the triplet one, produce always an antiferromagnetic contribution to the exchange coupling constant. At the DDCI1 level, the ionic/neutral ratio was calculated to be 0.66 and 0.41 in the $NH_3$ and $H_2O$ series, respectively. This observation may look counterintuitive at first since the calculated DDCI-1 $J$ values (Table 1) suggest a stronger antiferromagnetic behaviour in the $H_2O$ compounds. However, the presence of electron-withdrawing groups has

**Table 1** Calculated exchange coupling constants ($J$, in cm$^{-1}$) of the dinuclear models **EE**/**EO**, **EE**, **IS**, and **IL** in ammonia and water[a]

| | EE/EO | EE | IS | IL |
|---|---|---|---|---|
| CAS[2,2]SCF | 1.3/−0.8 | 0.0/0.0 | −0.1/−0.2 | −0.4 |
| CAS[2,2] + DDCI1 | 3.7/−3.9 | −0.1/0.0 | −0.4/−0.8 | −1.4 |
| CAS[2,2] + DDCI3 | 11.0/−12.7 | −0.9/−4.3 | −1.7/−5.3 | −3.3 |

[a] Left/right values correspond to $NH_3$/$H_2O$ as solvent. With $H_2O$, only one inter-chain dinuclear model was extracted from the crystal structure. Thus, values for **IL** are in ammonia.

 

been invoked as the origin of the decrease in the antiferromagnetic coupling in binuclear systems.[38] A possible explanation comes from the nephelexautic effects attributable to the $NH_3$ and $H_2O$ ligands. Indeed, due to the higher ligand field strength generated by $NH_3$ as compared to $H_2O$, the magnetic orbitals are expected to be more delocalized, resulting in a smaller on-site coulomb repulsion: the weight of the ionic forms increases as observed in the DDCI-1 calculations, and the antiferromagnetic contribution should be enhanced in the $NH_3$ derivative. In the mean time, the expansion of the magnetic orbitals leads an enhancement of the direct exchange, a ferromagnetic contribution which competes with the previous one. Therefore, the chemical modification induces deep changes not only in the molecular orbital shapes (diffuse character) but also in the constitution of the singlet wavefunctions (ionic *vs.* neutral). An antiferromagnetic shift is computed for the second intra-chain (**EE**) and inter-chain magnetic channels when replacing $NH_3$ by $H_2O$. Whatever the coordinated solvent, the role of the hydrogen-bond network in the inter-chain magnetic pathways seems to be of the same order of magnitude even if the number of weak contacts varies. Moreover, the role of the long **EE** intra-chain pathway evolves with the solvent nature with almost no interaction in the presence of ammonia and slight antiferromagnetic interactions with water. Clearly, the global antiferromagnetic behaviour of the title compound may be explained by an excess of $H_2O$ compared to $NH_3$ which is effectively found through the elemental analysis. One may also note that interpreting the magnetic data with only one $J$ value (as in Fig. 5) may be insufficient and that a more complex magnetic picture with entangled exchange channels may be considered.

## Conclusions

The original chain topology obtained with Cu(II) and azide ions in the presence of ammonia is characterized by X-ray diffraction. Due to the ammonia aqueous solution, the coordination sphere of the Cu(II) is completed by a statistical distribution of water and ammonia molecules giving rise to the general formula $\{Cu(\mu_{1,1,3}\text{-}N_3)(\mu_1\text{-}N_3)(NH_3)_{0.8}(H_2O)_{1.2}\}_n$. The $\mu_{1,1,3}$ coordination mode of the azide induces an unusual alternation of $\{Cu(\mu_{1,1}\text{-}N_3)(\mu_{1,3}\text{-}N_3)Cu\}$ **EE**/**EO** dimeric units. Electrochemical investigations evidence the reversibility of the Cu(II)/Cu(I) redox process and the stability of the Cu(I) phase. The magnetic properties are investigated through solid state characterization and *ab initio* multireference wavefunction calculations (DDCI). The experimental magnetic properties exhibit a global antiferromagnetic behaviour that can be explained by the highly asymmetric **EE**/**EO** coordination mode of the azide as well as non-negligible inter-chain interactions. The theoretical calculations based on the dense hydrogen-bond network confirm their strong involvement in the magnetic properties. This also has some repercussions on the second neighbour Cu···Cu interaction which is no longer negligible in the water derivative. Switching from ammonia to water enhances the antiferromagnetic behaviour by *ca.* $-23$ $cm^{-1}$. The combination of magnetic measurements and theoretical calculations strongly supports the presence of water molecules in agreement with the elemental analysis. This work contributes to enrich the class of azide complexes from the magnetic study point of view correlated to theoretical investigations as well as on the electrochemical aspect which is rarely approached in such systems. Further catalytic experiments are under study to take advantage of the stability of the Cu(I) species evidenced in the compound that presents a high number of active sites along the chain.

## Experimental part

### Synthesis

To a methanolic solution (5 mL) of $CuBr_2$, $2H_20$ (0,5 mmole, 130 mg) is added 4 equivalents of $NaN_3$ salt (2 mmoles, 130 mg) at room temperature. After 3 minutes stirring, a concentrated solution of $NH_3$ (25%) is added dropwise until the apparition of an intense blue colour characteristic of the presence of the Cu(II)–$NH_3$ complex. Single green crystals suitable for X-ray characterisation are obtained by slow evaporation.

### Single-crystal X-ray diffraction

Diffraction data sets are collected on an Oxford Gemini Diffractometer. Unit-cell parameters determination, data collection strategy and integration are carried out using the appropriate software. An empirical multi-scan absorption correction is applied to the data sets.[26a-c] All the structures are solved by direct methods using the SIR97 program[27] combined to Fourier difference syntheses and refined against F using reflections with $[I/\sigma(I) > 3]$ and using the CRYSTALS program.[28] All atomic displacement parameters for non-hydrogen atoms are refined using an anisotropic model. Hydrogen atoms have been found by Fourier Difference (see Fig. S2 in ESI† part) and then refined with a riding mode. CCDC 862144.†

Crystal structure: $T = 293$ K, system: orthorhombic, space group: *Pnma*; $a = 6.3808(3)$ Å, $b = 7.4452(3)$ Å, $c = 12.7044(5)$ Å, $V = 603.53(6)$ $Å^3$, $Z = 4$, crystal shape: needle, crystal colour: green, crystal size: $0.085 \times 0.089 \times 0.210$ $mm^3$, a total of 4545 reflections were collected, 810 unique ($R_{int} = 0.039$). Formula $Cu_1H_{4.8}N_{6.8}O_{1.2}$ ($H_2O/NH_3$ disorder), $M = 182.83$ g $mol^{-1}$, $\rho = 2.012$ g $cm^{-3}$, $\mu = 3.549$ $cm^{-1}$, $F(000) = 222$, $R/R_w = 0.0222/0.0256$, $S = 1.11$ with 56 refined parameters using 659 reflections. $\Delta\rho_{max}/\Delta\rho_{min} = 0.15/-0.35$ $e^-$ $Å^{-3}$.

### Electrochemistry

DMF solvents were purchased from Aldrich and used without further purification. Electrochemical measurements were performed using an AMEL 7050 all-in one potentiostat, using a standard three-electrode setup with a glassy carbon electrode (diameter 3 mm), a platinum wire auxiliary electrode and SCE (saturated calomel electrode) as a reference electrode. Concentrations of the solutions of complexes in DMF were 1.0 mM, 2 mM and 0.1 M with $n$-$Bu_4NPF_6$ as a supporting electrolyte (Fluka, electrochemical grade). Under these experimental conditions, the ferrocenium/ferrocene couple, used as an internal reference for potential measurements, was located at $E_{1/2} = 0.445$ V/SCE

### UV-Visible

The UV-Visible measurements were carried out using a Perkin Elmer Lambda 35 spectrometer. The spectro-electrochemistry

measurements were performed *in situ* during the electrolysis process with a special home electrochemical cell linked to a quartz cuvette (1 cm).

### Magnetic measurements

Magnetic measurements are performed on polycrystalline samples using a Quantum Design SQUID magnetometer MPMS-XL that works between 1.8 and 300 K for DC applied fields ranging from −5 to 5 T. The magnetic susceptibility is measured at 0.1 T. The magnetic data are corrected for the sample holder and diamagnetic contributions.

### Computational details

Complete active space self-consistent field (CASSCF)[29] calculations, including two electrons in two molecular orbitals (MOs), are performed on dinuclear units using the MOLCAS 7.2 package[30] to generate a reference space (CAS[2,2]), which consists of the configurations that qualitatively describe the problem. The dynamical correlation effects are then incorporated on top of the triplet CASSCF wavefunction by using the dedicated difference configuration interaction (DDCI)[31] method implemented in the CASDI code.[32] With this approach, one concentrates on the differential effects rather than on the evaluation of the absolute energies. Such a strategy is successfully used to study the magnetic properties of various molecular and extended materials.[5,33] All atoms are depicted with ANO-RCC type basis sets. The Cu atoms are described with a (21s15p10d6f4g2h)/[5s4p3d] contraction.[34] A (14s9p4d3f2g)/[3s2p] contraction is used for N and O,[35] whereas a minimal basis set (8s4p3d1f)/[1s] is used for the hydrogen atoms.[36] Let us mention that larger basis sets on Cu, N and O are also tested with no significant modifications on the calculated exchange coupling values. The robustness of the dimer picture was investigated by performing calculations on (intra-chain) trinuclear model complexes (CAS[3,3]) leading to similar conclusions.

## Acknowledgements

G.P., G.C. and B.L.G. thank the Région Rhône-Alpes (CIBLE 2009 ENAMBRIMOLE project) for financial support. G.P. thanks the ''Centre de Diffractométrie Henri Longchambon'', Université Claude Bernard Lyon 1 for the access to single-crystal X-ray diffractometers. B.L.G. and V.R. thank the Pôle Scientifique de Modélisation Numérique (PSMN) at ENS de Lyon for computing facilities. Patrick Rosa and Rodolphe Clérac are acknowledged for fruitful discussions and help with elemental analysis and interpretation of the magnetic data, respectively. Reviewers are acknowledged for pertinent comments.

## Notes and references

1 J. Ribas, A. Escuer, M. Monfort, R. Vicente, R. Cortes, L. Lezapma and T. Rojo, *Coord. Chem. Rev.*, 1999, **193**, 1027 and ref. therein.
2 J. Ribas, A. Escuer, M. Monfort, R. Vicente, R. Cortes, L. Lezama and T. Rojo and M. A. S. Goher, in *Magnetism: Molecules to Materials II: Molecule-Based Materials*, ed. J. S. Miller and M. Drillon, Wiley-VCH Verlag GmbH & Co. KGaA, Weinheim, 2002.
3 Y. F. Zeng, X. Hu, F.-C. Liu and X.-H. Bu, *Chem. Soc. Rev.*, 2009, **38**, 469.
4 C. Adhikari and S. Koner, *Coord. Chem. Rev.*, 2010, **254**, 2933.
5 G. Chastanet, B. Le Guennic, C. Aronica, G. Pilet, D. Luneau, M.-L. Bonnet and V. Robert, *Inorg. Chim. Acta*, 2008, **361**, 3847.
6 A. Escuer and G. Aromi, *Eur. J. Inorg. Chem.*, 2006, 4721.
7 (*a*) T.-F. Liu, D. Fu, S. Gao, Y.-Z. Zhang, H.-L. Sun, G. Su and Y.-J. Liu, *J. Am. Chem. Soc.*, 2003, **125**, 13976; (*b*) X.-T. Liu, X.-Y. Wang, W. X. Zhang, P. Cui and S. Gao, *Adv. Mater.*, 2006, **18**, 2852; (*c*) J. H. Yoon, D. W. Ryu, H. C. Kim, S. W. Yoon, B. J. Suh and C. S. Hong, *Chem.–Eur. J.*, 2009, **15**, 3661; (*d*) J. H. Yoon, J. W. Lee, D. W. Ryu, S. W. Yoon, B. J. Suh, H. C. Kim and C. S. Hong, *Chem.–Eur. J.*, 2011, **17**, 3028.
8 (*a*) Z. N. Chen, J. Qiu, Z. K. Wu, D. G. Fu, K. B. Yu and W. X. Tang, *J. Chem. Soc., Dalton Trans.*, 1994, 1923; (*b*) E.-Q. Gao, S.-Q. Bai, C.-F. Wang, Y.-F. Yue and C.-H. Yan, *Inorg. Chem.*, 2003, **42**, 8456; (*c*) M.-L. Bonnet, C. Aronica, G. Chastanet, G. Pilet, D. Luneau, C. Mathonière, R. Clérac and V. Robert, *Inorg. Chem.*, 2008, **47**, 1127; (*d*) A. M. Madalan, M. Noltemeyer, M. Neculai, H. W. Roesky, M. Schmidtmann, A. Müller, Y. Journaux and M. Andruh, *Inorg. Chim. Acta*, 2006, **359**, 459; (*e*) P. S. Mukherjee, T. K. Maji, G. Mostafa, T. Mallah and N. R. Chaudhuri, *Inorg. Chem.*, 2000, **39**, 5147; (*f*) P. S. Mukherjee, T. K. Maji, A. Escuer, R. Vicente, J. Ribas, G. Rasair, F. A. Mautner and N. R. Chaudhuri, *Eur. J. Inorg. Chem.*, 2002, 943; (*g*) G. De Munno, M. G. Lombardi, P. Paoli, F. Lloret and M. Julve, *Inorg. Chim. Acta*, 1998, **282**, 252.
9 (*a*) M. A. Halcrow, J. C. Huffman and G. Christou, *Angew. Chem., Int. Ed. Engl.*, 1995, **34**, 889; (*b*) M. A. Halcrow, J.-S. Sun, J. C. Huffman and G. Christou, *Inorg. Chem.*, 1995, **34**, 4167; (*c*) M. W. Wemple, D. M. Adams, K. S. Hagen, K. Folting, D. N. Hendrickson and G. Christou, *Chem. Commun.*, 1995, 1591; (*d*) D. Ma, S. Hikichi, M. Akita and Y. Morooka, *J. Chem. Soc., Dalton Trans.*, 2000, 1123; (*e*) M. A. S. Goher, J. Cano, Y. Journaux, M. A. M. Abu-Yussef, F. A. Mautner, A. Escuer and R. Vicente, *Chem.–Eur. J.*, 2000, **6**, 778.
10 (*a*) F. Meyer, S. Demeshko, G. Leibeling, B. Kersting and E. Kaifer, *Chem.–Eur. J.*, 2005, **11**, 1518; (*b*) S. Triki, C. J. Gomez-Garcia, E. Ruiz and J. Sala-Pala, *Inorg. Chem.*, 2005, **44**, 5501; (*c*) L. Zhang, L.-F. Tang, Z.-H. Wang, M. Du, M. Julve, F. Lloret and J.-T. Wang, *Inorg. Chem.*, 2001, **40**, 3619; (*d*) G. de Munno, M. G. Lombardi, M. Julve, F. Lloret and J. Faus, *Inorg. Chim. Acta*, 1998, **282**, 82; (*e*) L. Li, Z. Jiang, D. Liao, S. Yan, G. Wang and Q. Zhao, *Transition Met. Chem.*, 2000, **25**, 630; (*f*) T. K. Maji, P. S. Mukherjee, S. Koner, G. Mostafa, J.-P. Tuchagues and N. R. Chaudhuri, *Inorg. Chim. Acta*, 2001, **314**, 111; (*g*) A. Escuer, M. Font-Bardia, E. Penalba, X. Solans and R. Vicente, *Polyhedron*, 1999, **18**, 211; (*h*) Q.-F. Yang, Z.-G. Gu, C.-H. Li, J.-Q. Tao, J.-L. Zuo and X.-Z. You, *Inorg. Chim. Acta*, 2007, **360**, 2875; (*i*) F.-C. Liu, Y.-F. Zeng, J.-P. Zhao, B.-W. Hu, X.-H. Bu, J. Ribas and S. R. Batten, *Inorg. Chem. Commun.*, 2007, **10**, 129; (*j*) Z.-G. Gu, J.-L. Zuo and X.-Z. You, *Dalton Trans.*, 2007, 4067; (*k*) F. Meyer, P. Kircher and H. Pritzkow, *Chem. Commun.*, 2003, 774.
11 (*a*) G. S. Papaefstathiou, S. P. Perlepes, A. Escuer, R. Vicente and M. Font-Bardia, *Angew. Chem., Int. Ed. Engl.*, 2001, **40**, 884; (*b*) A. N. Georgopoulou, C. P. Raptopoulou, V. Psycharis, R. Ballesteros, B. Abarca and A. K. Boudalis, *Inorg. Chem.*, 2009, **48**, 3167.
12 (*a*) S. Demeshko, G. Leibeling, W. Maringgele, F. Meyer, C. Mennerich, H.-H. Klauss and H. Pritzkow, *Inorg. Chem.*, 2005, **44**, 519; (*b*) C. Golze, A. Alfonsov, R. Klingeler, B. Büchner, V. Kataev, C. Mennerich, H.-H. Klauss, M. Goiran, J.-M. Broto, H. Rakoto, S. Demeshko, G. Leibeling and F. Meyer, *Phys. Rev. B: Condens. Matter Mater. Phys.*, 2006, **73**, 2244031; (*c*) P. K. Nanda, G. Aromí and D. Ray, *Chem. Commun.*, 2006, 3181; (*d*) J. Peng Zhao, B.-W. Hu, E. C. Sanudo, Q. Yang, Y.-F. Zeng and X.-H. Bu, *Inorg. Chem.*, 2009, **48**, 2482.
13 For recent examples: (*a*) M. A. M. Abu-Youssef, M. Drillon, A. Escuer, M. A. S. Goher, F. A. Mautner and R. Vicente, *Inorg. Chem.*, 2000, **39**, 5022; (*b*) F.-C. Liu, Y.-F. Zeng, J.-P. Zhao, B.-W. Hu, X.-H. Bu, J. Ribas and J. Cano, *Inorg. Chem.*, 2007, **46**, 1520; (*c*) M. A. M. Abu-Youssef, A. Escuer, M. A. S. Goher, F. A. Mautner, G. J. Reiss and R. Vicente, *Angew. Chem., Int. Ed. Engl.*, 2000, **39**, 1624; (*d*) F.-C. Liu, Y.-F. Zeng, J.-P. Zhao,

 

B.-W. Hu, X.-H. Bu, J. Ribas and J. Cano, *Inorg. Chem.*, 2007, **46**, 1520.
14 (*a*) J. Ribas, M. Monfort, C. Diaz, C. Bastos and X. Solans, *Inorg. Chem.*, 1993, **32**, 3557; (*b*) R. Vicente and A. Escuer, *Polyhedron*, 1995, **14**, 2133; (*c*) A. Escuer, R. Vicente, M. A. S. Goher and F. A. Mautner, *Inorg. Chem.*, 1998, **37**, 782; (*d*) R. J. Butcher, C. J. O'Connor and E. Sinn, *Inorg. Chem.*, 1981, **20**, 3486; (*e*) T. K. Karmakar, B. K. Ghosh, A. Usman, H. K. Fun, E. Riviere, T. Mallah, G. Aromí and S. K. Chandra, *Inorg. Chem.*, 2005, **44**, 2391; (*f*) A. Escuer, M. Font-Bardia, S. S. Massoud, F. A. Mautner, E. Penalba, X. Solans and R. Vicente, *New J. Chem.*, 2004, **28**, 681.
15 (*a*) E. Ruiz, J. Cano, S. Alvarez and P. Alemany, *J. Am. Chem. Soc.*, 1998, **120**, 11122; (*b*) F. Fabrizi di Biani, E. Ruiz, J. Cano, J. J. Novoa and S. Alvarez, *Inorg. Chem.*, 2000, **39**, 3221; (*c*) O. Castell, R. Caballol, V. M. Garcia and K. Handrick, *Inorg. Chem.*, 1996, **35**, 1609; (*d*) J. Cabrero, C. de Graaf, E. Bordas, R. Caballol and J.-P. Malrieu, *Chem.–Eur. J.*, 2003, **9**, 2307.
16 (*a*) C. Aronica, E. Jeanneau, H. El Moll, D. Luneau, B. Gillon, A. Goujon, A. Cousson, M. A. Carvajal and V. Robert, *Chem.–Eur. J.*, 2007, **13**, 3666; (*b*) M. A. Carvajal, C. Aronica, D. Luneau and V. Robert, *Eur. J. Inorg. Chem.*, 2007, **28**, 4434; (*c*) Q.-X. Jia, M.-L. Bonnet, E.-Q. Gao and V. Robert, *Eur. J. Inorg. Chem.*, 2009, 3008.
17 G. Pilet, M. Medebielle, J.-B. Tommasino, G. Chastanet, B. Le Guennic and C. Train, *Eur. J. Inorg. Chem.*, 2009, 4718.
18 J.-B. Tommasino, F. N. Renaud, D. Luneau and G. Pilet, *Polyhedron*, 2011, **30**, 1663.
19 (*a*) A. Escuer, R. Vicente, M. S. El Fallah, M. A. S. Goher and F. A. Mautner, *Inorg. Chem.*, 1998, **37**, 4466; (*b*) F. A. Mautner and M. A. S. Goher, *Polyhedron*, 1995, 1809; (*c*) S. Martin, M. G. Barandika, L. Lezama, J. L. Pizarro, Z. E. Serna, J. I. Ruiz de Larramendi, M. I. Arriortua, T. Rojo and R. Cortes, *Inorg. Chem.*, 2001, **40**, 4109.
20 (*a*) E. I. Solomon, R. K. Szilagyi, S. D. George and L. Basumallick, *Chem. Rev.*, 2004, **104**, 419; (*b*) D. B. Rorabacher, *Chem. Rev.*, 2004, **104**, 651.
21 (*a*) M. R. DeFelippis, M. Faraggi and M. H. Klapper, *J. Phys. Chem.*, 1990, **94**, 2420; (*b*) Z. B. Alfassi, A. Harriman, R. E. Huie, S. Mosseri and P. Neta, *J. Phys. Chem.*, 1987, **91**, 2120; (*c*) S. Sarkar, A. Mondal, J. Ribas, M. G. B. Drew, K. Pramanik and K. K. Rajak, *Eur. J. Inorg. Chem.*, 2004, 4633; (*d*) P. Bhunia, D. Banerjee, P. Datta, P. Raghavaiah, A. M. Z. Slawin, J. D. Woolins, J. Ribas and C. Shina, *Eur. J. Inorg. Chem.*, 2010, 311; (*e*) I. Banerjee, J. Marek, R. Herchel and M. Ali, *Polyhedron*, 2010, **29**, 1201.
22 (*a*) O. Kahn, *Molecular Magnetism*, VCH, New York, 1993; (*b*) W. E. Estes, D. P. Gavel, W. E. Hatfield and D. J. Hodgson, *Inorg. Chem.*, 1978, **17**, 1415.
23 (*a*) S. Koner, S. Saha, T. Mallah and K.-I. Okamoto, *Inorg. Chem.*, 2004, **43**, 840; (*b*) M. S. Ray, A. Ghosh, S. Chaudhuri, M. G. B. Drew and J. Ribas, *Eur. J. Inorg. Chem.*, 2004, 3110.
24 I. Seggern, F. Tuczek and W. Bensch, *Inorg. Chem.*, 1995, **34**, 5530.
25 (*a*) S. S. Tandon, L. K. Thompson, M. E. Manuel and J. N. Bridson, *Inorg. Chem.*, 1994, **33**, 5555; (*b*) L. K. Thompson, S. S. Tandon and M. E. Manuel, *Inorg. Chem.*, 1995, **34**, 2356.
26 (*a*) CrysAlisPro, Oxford Diffraction Ltd., Version 1.171.34.40 (release 27-08-2010 CrysAlis171.NET); (*b*) Nonius, Nonius B. V., Delft, The Netherlands, Editon edn., 1999; (*c*) CrysAlisPro, Oxford Diffraction Ltd., Version 1.171.33.46 (release 27-08-2009 CrysAlis171.NET); empirical absorption correction using spherical harmonics, implemented in the SCALE3 ABSPACK scaling algorithm.
27 G. Cascarano, A. Altomare, C. Giacovazzo, A. Guagliardi, A. G. G. Moliterni, D. Siliqi, M. C. Burla, G. Polidori and M. Camalli, *Acta Crystallogr.*, 1996, A52–C79.
28 P. W. Betteridge, J. R. Carruthers, R. I. Cooper, K. Prout and D. J. Watkin, *J. Appl. Crystallogr.*, 2003, **36**, 1487.
29 B. O. Roos, *Adv. Chem. Phys.*, 1987, **69**, 399.
30 G. Karlstrom, R. Lindh, P. A. Malmqvist, B. O. Roos, U. Ryde, V. Veryazov, P. O. Widmark, M. Cossi, B. Schimmelpfennig, P. Neograd y and L. Seijo, *Comput. Mater. Sci.*, 2003, **28**, 222.
31 (*a*) J. Miralles, J. P. Daudey and R. Caballol, *Chem. Phys. Lett.*, 1992, **198**, 555; (*b*) J. Miralles, O. Castell, R. Caballol and J. P. Malrieu, *Chem. Phys.*, 1993, **172**, 33.
32 N. Ben Amor and D. Maynau, *Chem. Phys. Lett.*, 1998, **286**, 211.
33 For instance: (*a*) D. Herebian, K. E. Wieghardt and F. Neese, *J. Am. Chem. Soc.*, 2003, **125**, 10997; (*b*) S. Messaoudi, V. Robert, N. Guihéry and D. Maynau, *Inorg. Chem.*, 2006, **45**, 3212; (*c*) C. de Graaf and F. Illas, *Phys. Rev. B: Condens. Matter Mater. Phys.*, 2001, **63**, 014404; (*d*) F. Illas, I. de P. Moreira, C. de Graaf and V. Barone, *Theor. Chem. Acc.*, 2000, **104**, 265; (*e*) B. Le Guennic, S. Petit, G. Chastanet, G. Pilet, D. Luneau, N. Ben Amor and V. Robert, *Inorg. Chem.*, 2008, **47**, 572; (*f*) B. Le Guennic, N. Ben Amor, D. Maynau and V. Robert, *J. Chem. Theory Comput.*, 2009, **5**, 1506; (*g*) J. S. Costa, N. A. G. Bandeira, B. Le Guennic, V. Robert, P. Gamez, G. Chastanet, L. Ortiz-Frade and L. Gasque, *Inorg. Chem.*, 2011, **50**, 5696.
34 B. O. Roos, R. Lindh, P. A. Malmqvist, V. Veryazov and P. O. Widmark, *J. Phys. Chem. A*, 2005, **109**, 6575.
35 B. O. Roos, R. Lindh, P. A. Malmqvist, V. Veryazov and P. O. Widmark, *J. Phys. Chem. A*, 2004, **108**, 2851.
36 P. O. Widmark, P. A. Malmqvist and B. O. Roos, *Theor. Chim. Acta*, 1990, **77**, 291.
37 O. Oms, J.-B. Rota, L. Norel, C. J. Calzado, H. Rousselière, C. Train and V. Robert, *Eur. J. Inorg. Chem.*, 2010, 5373.
38 D. Venegas-Yazigi, D. Aravena, E. Spodine, E. Ruiz and S. Alvarez, *Coord. Chem. Rev.*, 2010, **254**, 2086; L. K. Thompson, S. K. Mandal, S. S. Tandon, J. N. Bridson and M. K. Park, *Inorg. Chem.*, 1996, **35**, 3117; S. K. Mandal, L. K. Thompson, M. J. Newlands, E. J. Gabe and K. Nag, *Inorg. Chem.*, 1999, **29**, 1324.